DUCT WALL BREAKOUT: FRIEND OR FOE?

Alan Cummings Department of Engineering, University of Hull

1 INTRODUCTION

Acoustic “breakout” from ducts is a result of sound radiation from elastic or acoustically permeable porous duct walls, with solid or fluid motion in the walls excited by an internal sound field. There are various situations in which breakout noise can be a problem. For example sheet metal HVAC ductwork, passing through ceiling voids above internal building spaces, can radiate noise into the occupied spaces beneath and thereby create disturbance to whomever is present. Even if the noise propagating internally within the duct is broadband in nature, the radiated noise may have significant (usually low frequency) narrow-band components related to structural resonances in the duct walls, and this can exacerbate the intrusiveness of the breakout component. Despite the importance of breakout noise in HVAC acoustics, it was not studied in any detail until the late 1970s onward. Prior to that time Allen[1] had given a simple analysis of noise transmission both out of, and into, a duct in a reverberant space (only really applicable at high frequencies), Webb[3] had given a good general account of breakout and Sharland[2] had briefly discussed the significance of breakout in HVAC ducts, including Allen’s breakout formula. Since the breakout sound transmission loss of duct walls (apart from those of circular cross-section) is usually lowest at low frequencies and the internal sound power spectral density normally rises with falling frequency, breakout noise in HVAC ducts is predominantly a low frequency problem. It often sounds subjectively like a “rumble”.

Another example of breakout is noise radiation from piping downstream of pressure control valves, but here the internal sound power spectrum tends to peak at high frequencies and the pipe is invariably circular in cross-section, so the radiated noise is mainly high frequency in content, with peaks around the ring frequency and the critical frequency of the pipe wall. Multi-mode mode sound propagation in the duct is associated with control valve noise radiation from piping. HVAC duct wall breakout usually arises principally from fan noise, whereas pressure control valve noise is caused predominantly by mixing noise in the jet formed downstream of the valve. For these reasons, valve noise as a technical area is usually regarded as being distinct from HVAC duct breakout noise. Though it constitutes a widespread and very significant noise problem, valve noise will be largely excluded from the present discussion (which mainly centres round HVAC duct noise breakout) because it has not been of specific interest to the author in his research. However, it could certainly be included as a breakout problem in a more general context.

“Casing noise” in automotive exhaust silencers is a further example of noise breakout. Here, the dominant noise source is engine breathing noise and it is structural vibration of the silencer casing – driven by the internal sound field – that radiates noise to the exterior. Silencer casings are often circular or oval in cross-section, though more complex wall geometries (e.g., the “clam-shell” configuration) also exist. Casing noise in silencers has been less widely studied than HVAC breakout noise or valve noise, and appears to be less well quantified. It would seem likely to be most important at mid to high frequencies, though this author is prepared to stand corrected in the light of more definite information. It would seem, in view of the strongly tonal content of breathing noise, that casing noise would become important when one of the harmonics of the noise source corresponded to a resonance frequency of the silencer casing. Therefore one would expect it to appear and disappear as the engine speed and load varied. As with valve noise, silencer casing noise is not discussed in any detail in this paper.

"Flanking" effects in dissipative silencers can be partly caused by breakout and subsequent "breakin" through flexible duct walls, thus limiting the performance of the silencer. These effects are not very well understood, quantitatively, even today and can be an important and unpredictable factor in silencer design.

Breakout noise is generally regarded as being a problem, but there are cases in which it can be of benefit. Notably, in HVAC acoustics, there is "natural duct attenuation", that occurs in *unlined* ducts. This has been reported by a number of authors (e.g., Wilbur and Simmons[4], Piestrup and Wesler[5] and Kerka[6]) with no real attempt at properly identifying and quantifying the attenuation mechanism, but has been modelled by the present author[7] with modest success. In this work, a breakout/breakin mechanism was held to be responsible for the attenuation phenomenon, and the acoustic characteristics of the surrounding space (as well as the construction of the duct walls) were shown to be factors determining the degree of attenuation. Natural duct attenuation is an unavoidable phenomenon in plain sheet metal ducting, but it can be exploited by careful design and will complement the (usually meagre) attenuation afforded by dissipative silencers at low frequencies. It reaches maxima in the region of transverse resonance frequencies of the duct walls.

Another manifestation of duct wall breakout which can have a beneficial effect occurs in ducts with walls that are permeable to fluid flow. The porous, woven fabric hoses that have become popular in recent years as components of automotive air intake systems are of this type. There are two main effects associated with these hoses: acoustic breakout, such that a proportion of the internally propagated intake breathing noise from the engine is transmitted out through the duct walls upstream of the air inlet; and acoustic dissipation, such that a very significant proportion of the incident internal sound power is actually dissipated in the duct walls. These effects will be discussed in more detail later in this paper.

The main purpose of this paper is to present both the disadvantageous and useful effects of duct wall breakout side by side, and to highlight the main physical effects responsible for the phenomena involved, as well as outlining predictive methods for breakout. Mathematics will be avoided as far as possible, so as not to encumber the discussion unduly with formulae. Full details of the various types of analysis employed in past studies are given in many of the references cited here.

2 DUCT WALL BREAKOUT AS A PROBLEM

2.1 Definitions and assumptions

In Figure 1 is shown a sound wave (for the sake of argument, depicted as plane), propagating internally in a duct, *in one direction only*. The walls may be either elastic and impermeable, or permeable and rigid (again for the sake of argument). In either case, "breakout" sound will radiate from the duct walls, and usually the direction of propagation of this will be neither normal to, nor parallel to, the duct walls. In practice, the radiation pattern would be complex in nature, since the duct would be of finite length, possibly with stiffening elements which could give rise to significant reflected waves. However, this idealised picture is appropriate for a definition of breakout sound transmission loss (TL):

$$TL = 10 \log[(W_i/A_i)/(W_r/A_r)], \qquad (1)$$

where

W_i = sound power entering duct
W_r = sound power radiated by duct walls
A_i = internal duct cross-sectional area
A_r = radiating area of duct surface.

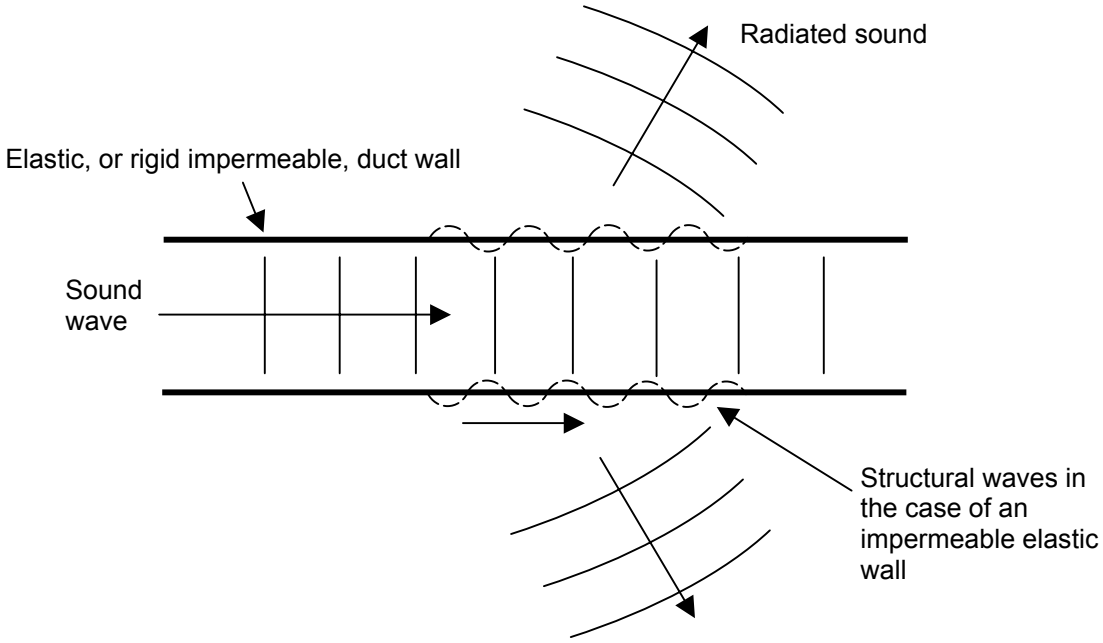

Figure 1. Breakout from a duct

The breakout sound power W_r may be radiated into a free field or (say) a reverberant space. Other breakout definitions are, of course, possible, but that above appears to be the most popular.

In the case of breakout from flexible-walled ducts it is generally sufficient to assume that there is only one wave propagating, in the direction away from the noise source. Reflections will, of course, occur in practice but these would normally be relatively weak (depending on the duct configuration) and can be ignored as a first approximation. Furthermore, it may be assumed that structural waves – in the duct walls – and acoustic waves – within the duct – travel at the same speed, with an axial wavenumber k_x (in the x direction). We can, therefore, say that (*pressure, displacement* etc.) $\propto \exp(-ik_x x)$, if x points away from the source. Thus *coupled* waves are assumed to exist and k_x needs, strictly speaking, to be found from a dispersion equation that embodies both acoustic and structural wave motion. Reflections of coupled waves from discontinuities would generally be highly complex in nature, since a set of coupled waves will normally exist and these would be required to satisfy several structural and acoustic matching conditions at each discontinuity. One possible example of a discontinuity is a relatively massive and stiff flange in an otherwise continuous sheet metal duct. This is likely to present little impediment to the acoustic wave, but would be a significant reflector of the structural wave. Structural reflections would be mainly in coupled modes that strongly resembled free structural wave modes, with little structural/acoustic coupling. At low frequencies (well below the critical frequency for wave coincidence for the duct wall material), these modes would travel slowly and radiate little sound power. They could be termed “acoustically slow” (as in plate modes) and would radiate sound very inefficiently. This is one reason why the single coupled travelling-wave assumption is justified. In all of what follows, mean fluid flow is neglected. This has been included in a numerical formulation by Kirby[8] for lined rectangular ducts, but its effects are small for low mean flow Mach numbers.

2.2 The prediction of breakout *TL* in ducts with flexible walls

There are essentially three parts to the prediction of breakout *TL* in flexible-walled ducts:

(1) calculation of the structural response of the duct walls for a given internal sound field
(2) calculation of the radiation efficiency of the walls, and hence of the breakout sound power

(3) calculation of the breakout *TL* from W_r, W_i (found from the internal sound field) and the *TL* definition in equation (1).

2.2.1 The structural response of the walls

The calculation of the wall response depends very much on the cross-sectional geometry of the duct walls (this is assumed uniform along the length of the duct), and on the nature of the internal sound field. The three most common duct shapes are shown in Figure 2. In rectangular ducts, the

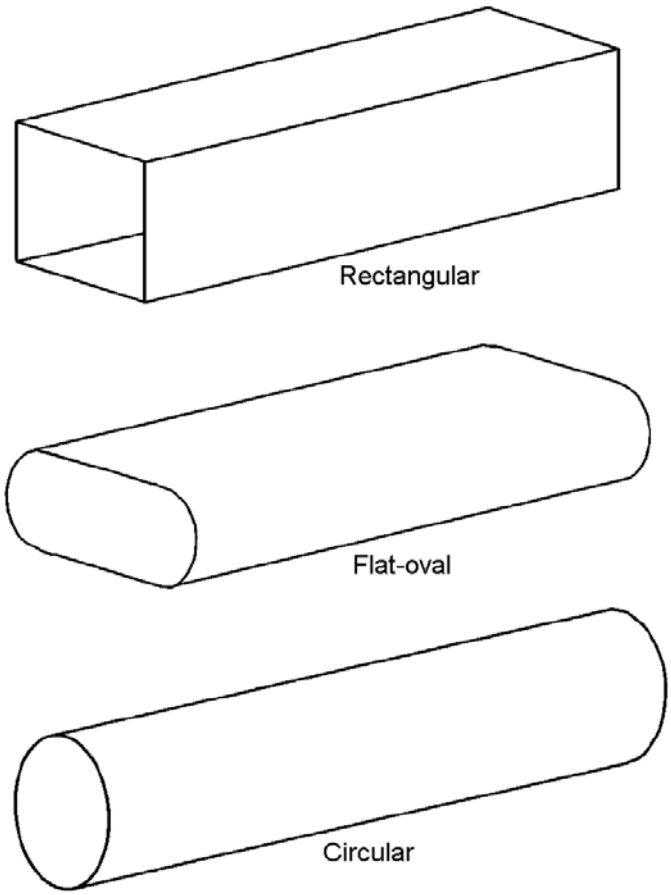

Figure 2. Common shapes of HVAC duct

response may be found by solving the inhomogeneous equation of motion for each wall (which is regarded as being a flat plate), with appropriate coupling conditions at the four corners. The forcing function is the internal/external sound pressure differential, either for the fundamental acoustic mode or for higher order modes. In the former case, it is straightforward to include coupling effects between the internal sound field and the structure, and to compute k_x. In the latter case, it is neither so simple nor particularly necessary. Either approximate analytical techniques, or fully numerical methods such as finite differences[9] or finite elements[10], may be employed. Peaks in the wall response, corresponding to transverse structural resonances of the duct walls (taken all together, and usefully viewed as a set of coupled beams formed by taking a transverse slice from the duct), occur at certain frequencies. These are associated with minima in the breakout *TL* of the duct. Structural damping in the duct wall may be taken into account in the form of the imaginary part of a complex Young's modulus of the duct wall material. A mass law model for the wall response works well, above the region of the lowest transverse wall resonances, much as it does in the case of sound transmission through single flat partitions.

In ducts having a circular (or distorted circular) cross-section, the equations of motion to be solved are those for a non-circular cylindrical shell, e.g. the inhomogeneous Reissner-Naghdi-Berry equations or the Donnell-Mushtari equations, with a forcing term representing the internal/external sound pressure difference across the shell surface. (In the case of circular section ducts, these equations simplify considerably.) Cummings, Chang and Astley[11] solved the Reissner-Naghdi-Berry equations by the use of a Fourier series method. This method proved reasonably successful in predicting the wall transmission loss for the plane internal acoustic mode in the case of two distorted circular "long-seam" ducts (galvanized steel ducts with a longitudinal seam, associated with a degree of flattening of the wall). The main effect of wall distortion is to increase the structural response of the duct wall considerably, at low to mid frequencies, as compared to an ideally circular section shell. This effect arises from what has been termed "mode coupling" and the reader is referred also to other authors' work such as that by Bentley and Firth[12] and Yousri and Fahy[13] for further discussion. In the case of the plane mode propagating within a distorted cylindrical shell, the effect involves a series of higher structural modes, in the duct wall, being excited by an internal uniform sound pressure distribution: the wall distortion produces a non-zero generalized force for the higher modes of the duct wall. In distorted circular ducts, maxima occur in the wall response at the ring frequency and the critical frequency for wave coincidence, as in undistorted ducts.

In the case of flat-oval section ducts (which have two opposite flat sides and two opposite circularly curved sides), a simplistic view of the wall response behaviour might be that a combination of the behaviours of flat-walled and circular ducts would be expected. Perhaps surprisingly, this is what occurs in practice. The response of the flat parts of the wall increases with frequency much as it does in the case of a duct of rectangular cross-section, and a maximum response occurs close to the ring frequency in the curved parts of the wall. A simple model for the wall response involves a combination of mass law impedance for the flat walls and ideal circular duct wall impedance for the curved walls. This has been used by Cummings and Chang[15] and yields reasonable breakout *TL* predictions for the plane internal duct mode. In the same paper, results from a finite difference solution to the Reissner-Naghdi-Berry non-circular cylindrical shell equations – applied to the flat-oval duct geometry – are also presented. Not surprisingly, the numerical solution yields rather better *TL* predictions than the simpler model, but the simplicity of the latter is a virtue in practical terms.

It will be recalled that it is the sound pressure *differential* across the duct wall that forces the wall motion, and at first sight it would therefore appear that the sound pressure on the outer surface of the duct should be a necessary part of the *TL* formulation. However, it was shown by Astley and Cummings[10] that the external radiation load on the duct walls is negligible in comparison to the wall impedance, including structural damping. There is therefore no need to include the radiation impedance in the *TL* prediction method. It should be noted that the acoustic radiation models in Section 2.2.2 are intended for forecasting the *far-field* sound pressure distribution (and the associated breakout sound power) and, and would – as they stand – be incapable of predicting of the sound pressure on the outer surface of the duct. If it were required to predict the outer surface sound pressure distribution, the formulation employed by Cummings and Kirby[16], involving the mutual radiation impedances of area elements of the outer duct surface, could be used.

2.2.2 Sound radiation from the walls

At relatively low frequencies, the finite-length line source model of Brown and Rennison[17] yields good predictions of sound radiation, as discussed by Cummings[18]. This involves "peristaltic" structural waves travelling along a finite-length source, and the effective volume velocity amplitude per unit length can be found simply by integrating the wall velocity around the duct perimeter. It is usually sufficient to consider waves travelling in one direction only, but wave reflections can readily be included if necessary. This model gives good results for both the free-field directivity pattern of the acoustic radiation and the radiation efficiency. The sound power radiated is dependent on the phase speed of the peristaltic waves and on the duct length, as well as on the volume velocity amplitude per unit length of duct. In a source of infinite length, no sound is radiated for subsonic structural waves, though the source begins to radiate efficiently as soon as the wave speed becomes supersonic. In the case of a finite length source, scattering effects brought about by the ends of the duct bring about a more gradual change in radiating ability, and finite sound power is

radiated for subsonically propagating waves. A "radiation efficiency" factor C_r may be defined as the sound power radiated, per unit length of source, from a finite length line source (with a given wave speed, frequency and volume velocity per unit length) divided by the sound power radiated, per unit length, from an infinite line source with supersonically travelling waves (the other conditions being identical to those in the finite-length source). The model of Brown and Rennison shows that, provided the duct length is greater than about an acoustic wavelength, for *sonically* propagating waves (which would be roughly characteristic of duct wall vibration away from wall resonance frequencies, where the structural wave speed along the duct could be either much less than, or much greater than, the sound speed), $C_r \approx 0.5$. This is a good assumption for sound radiation from duct walls, but would break down near to wall resonance frequencies.

In the case of higher circumferential order structural mode radiation from duct walls, where the net volume velocity around the duct perimeter would be zero, the simple low frequency line source model fails since it predicts zero sound radiation, whereas it is observed in practice that circumferential multipole radiation occurs, with an efficiency that increases with frequency. This situation can arise in the case of higher order internal acoustic mode propagation in flexible walled ducts, or – at high frequencies – in any case of duct wall radiation where the wall vibration amplitude is perimetrally non-uniform, and the higher order circumferential Fourier components of the wall vibration pattern can radiate significantly. A more complete model is therefore required for such cases. It is usually sufficient to approximate the duct cross-section as being circular, with the same perimeter as the actual duct, the actual perimetral vibration pattern being distributed around the circumference of the equivalent circular section radiator. A suitable finite-length radiator model of this type is described by Cummings, Chang and Astley[11], and consists of an infinite-length rigid cylinder with a finite-length vibrating section, the two remaining semi-infinite regions of cylinder being immobile. It is shown by Astley in this paper that the end extensions on the cylinder make little difference to the acoustic radiation, so that their presence may be ignored. In any case, one can argue that they should be present, if one is considering radiation from a finite section of continuous ducting. A detailed numerical study of sound radiation from rectangular ducts by Astley (reported in the paper by Astley and Cummings[10]) provides justification for the use of the simple line source model in the case of rectangular ducts with a plane internal acoustic mode.

2.2.3 Calculation of the internal and radiated sound power, and the *TL*

The internal sound power in the duct may conveniently be expressed

$$W_i = \frac{\mathrm{Re}(k_x)|P_i|^2}{2\omega\rho} \iint_{A_i} |\Psi(\mathbf{y})|^2 \, dA_i \,, \qquad (2)$$

where the axial wavenumber k_x in the duct may be complex, as it would be in the case of walls with internal damping, ω is the radian frequency, ρ is the air density, A_i is (as before) the internal cross-sectional areas of the duct and $P_i \Psi(\mathbf{y})$ is the internal sound pressure distribution (where P_i is a constant sound pressure), **y** being a relative position vector on the duct cross-section. The radiated sound power may be expressed

$$W_r = C_r \omega \rho |q|^2 L / 8 \qquad (3)$$

if a line source model is being used, where q is the volume velocity per unit length on the outer surface of the duct and L is the radiating length of the duct. If the aforementioned cylindrical radiator model is used, a modal summation of sound power contributions would be required. The interested reader is referred, for details of this, to the work of Cummings, Chang and Astley[11] and also of Cummings[19], where a simpler cylindrical radiator model – applied to internal higher order acoustic mode excitation of duct walls – is described. The breakout *TL* may be found, from W_i and W_r, by the use of equation (1).

2.2.4 Some typical *TL* results for ducts with differing cross-sectional shapes

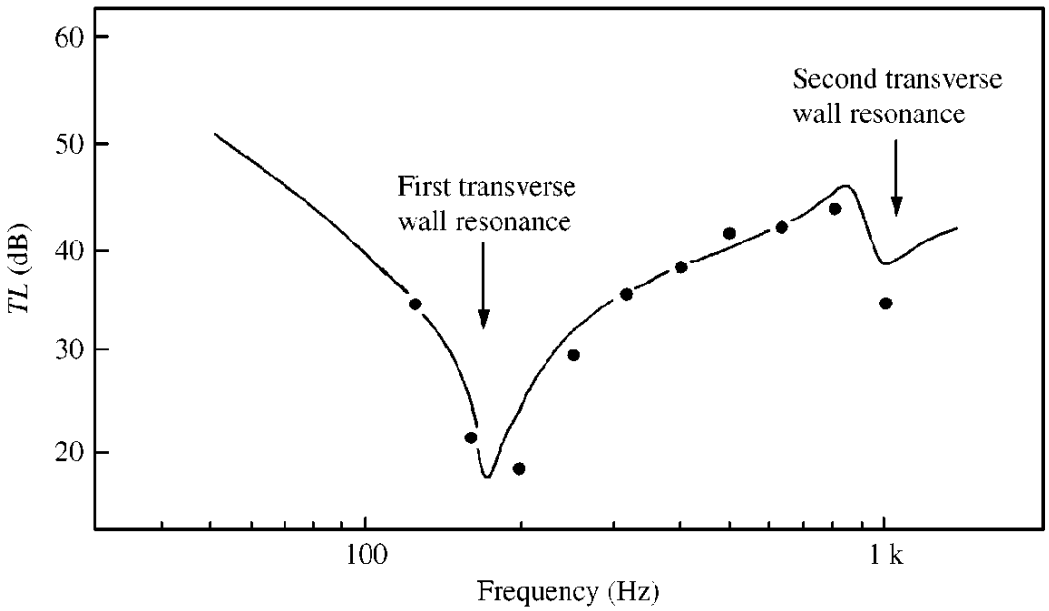

Figure 3. Predicted, ——, and measured, ●, *TL* of a 203mm square section duct with 1.2mm steel walls

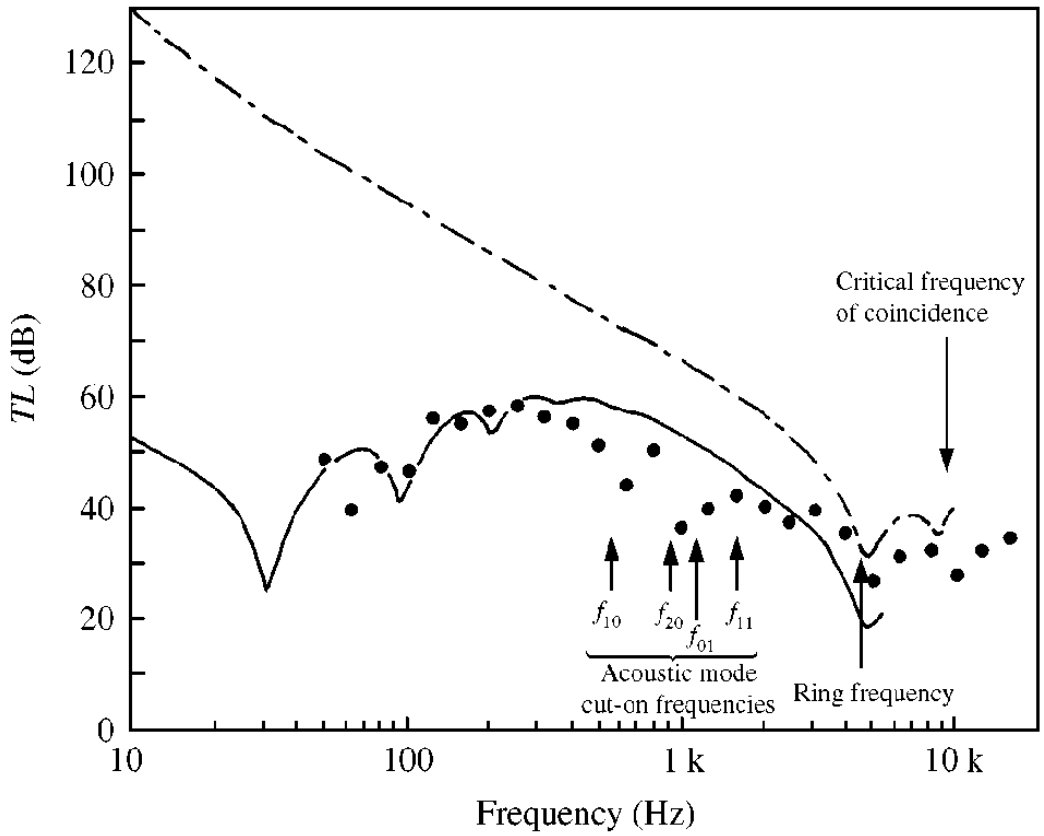

Figure 4. Predicted, ——, and measured, ●, *TL* of a 356mm diameter long-seam distorted circular duct with 1.2mm galvanized steel walls; — - —, predicted *TL* of ideally circular duct.

A good example of the *TL* of a rectangular duct is shown in Figure 3. Here, the duct cross-section is square, and there is a fundamental transverse wall resonance leading to a very pronounced dip in the *TL* curve at 170 Hz. This is so marked that internally propagated broadband noise within the experimental duct gave rise to breakout noise having a predominantly tonal character. Below the fundamental wall resonance, the *TL* rises with falling frequency, since the duct wall impedance is then stiffness controlled. The second transverse wall resonance at 1 kHz produces a much less severe dip in *TL*. It may be noted that the predicted and measured *TL* figures are in generally good agreement, and that a rather high wall loss factor of the order of 0.15 is required to give good agreement between prediction and experiment around resonance frequencies.

In rectangular ducts generally, above about the second transverse wall resonance, the *TL* increases at roughly 3 dB per doubling of frequency in the plane-wave propagation frequency region, rising to 6 dB per octave where many modes propagate in the duct. This is discussed in detail by Cummings[20], who proposed fairly simple mass law *TL* models that yield generally satisfactory predictions.

The predicted and measured *TL* of a "long-seam" distorted circular section duct is shown in Figure 4. The continuous curve is predicted by the use of the Fourier series model mentioned in Section 2.2.1, and the dashed and dotted curve is predicted for an ideally circular section duct with the same diameter. It can be seen that wall distortion brings about an enormous fall in *TL* – amounting to about 80 dB at just over 30 Hz – at the lower frequencies. This effect is caused by mode coupling, as previously mentioned. At the higher frequencies, where the ideally circular duct *TL* falls to fairly low values, there is a much lesser effect from wall distortion. The predicted *TL* plots are both made on the basis of the plane internal acoustic mode, and – not surprisingly – some *TL* minima are observed in the measured data around the cut-on frequencies of the first few higher order acoustic modes in the duct. The ring frequency resonance and the wave coincidence effect persist, even in the presence of wall distortion.

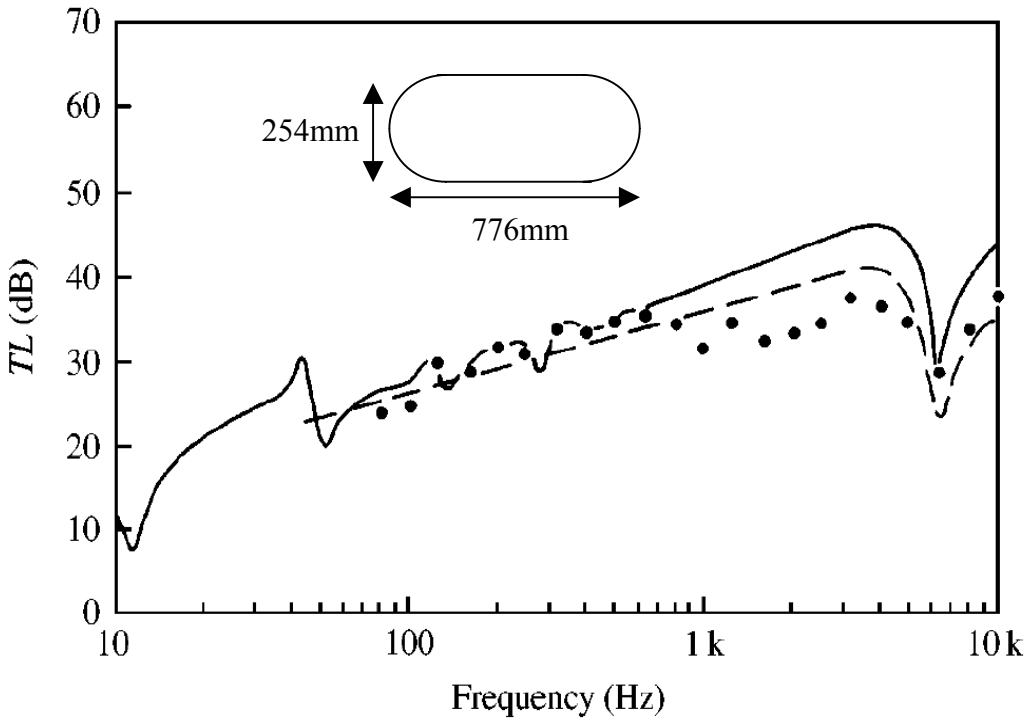

Figure 5. Predicted, —— (finite difference), — — (circular cylinder/flat plate model), and measured, ●, *TL* of a 254mm×776mm flat-oval duct with 0.64mm galvanized steel walls.

In Figure 5 is shown the *TL* of a flat-oval duct. This may be regarded as an extreme case of a distorted circular section duct. The solid curve is predicted by the use of a finite difference solution for the wall vibration, and is in good agreement with measured data up to about 700 Hz. Above that frequency, higher-order mode propagation within the duct brings about discrepancies between prediction and measurement, since the predictions are made on the basis of the plane internal acoustic mode. The much simpler hybrid prediction method, based on a combination of flat plate mass law for the flat walls and ideal circular duct wall impedance for the curved walls, is in reasonable agreement with measured data. Transverse wall resonances appear in the finite difference *TL* plot, and so does the ring frequency resonance. It is interesting that the flat-oval duct exhibits characteristics of both rectangular and circular ducts. The positive slope of the *TL* curve below about 4 kHz may be regarded as an extension of the mode-coupling behaviour evident in the distorted circular duct. In this case, the wall distortion is such that the radius of curvature of each flat wall is infinite, and flat-plate behaviour dominates the *TL* in this frequency range.

2.3 Flanking transmission in rectangular ducts

It is well known that "flanking transmission" can limit the performance of duct silencers. Vér[21] noted that, as the length of a dissipative duct liner in a sheet metal duct was increased, the acoustic attenuation of the liner tended to level off at a certain point, and speculated that this may have been caused by "...bending waves travelling in the duct wall...". Mechel[22] distinguished between breakout/breakin flanking transmission (which he termed a "radiation bypass") and direct structural flanking transmission through the silencer housing or the supporting structure of sound-absorbing baffles (which he termed "structure-borne sound"). He recognized that these effects would limit the attenuation of high-performance silencers, and "...must be avoided very carefully".

Cummings and Astley[23] later presented a model for flanking effects in an acoustically lined duct with flexible walls, situated within a reverberant enclosure. Both radiation bypass and direct structural flanking mechanisms are incorporated in this model, and the roles of both in limiting the attenuation of the duct lining were demonstrated. This model will be briefly described in the next section.

2.3.1 A predictive model

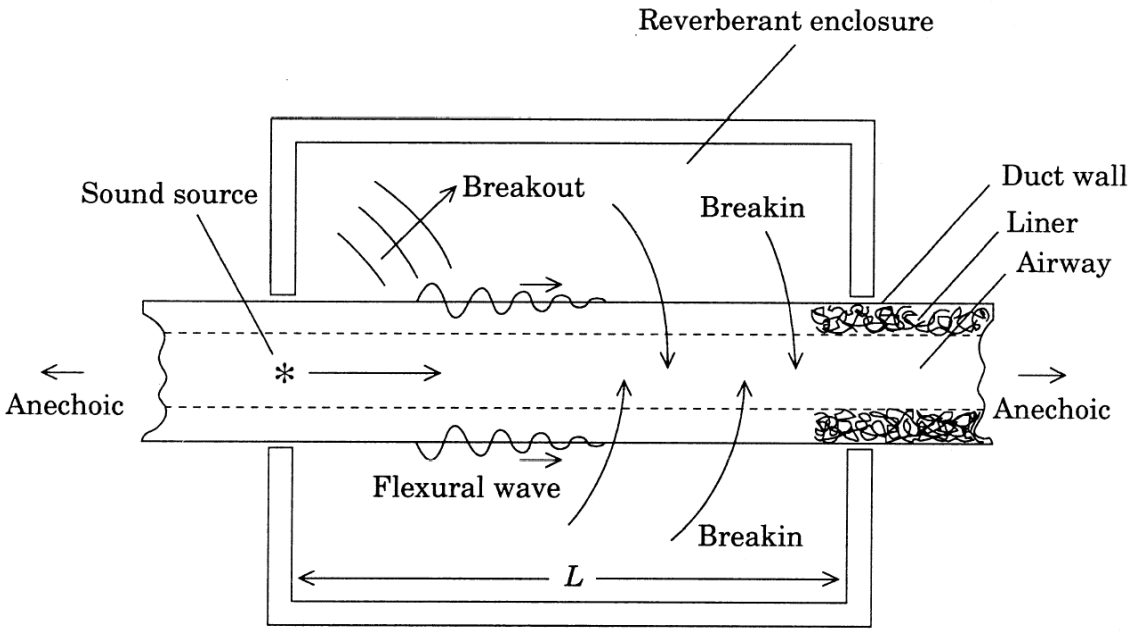

Figure 6. An acoustically lined duct in a reverberant enclosure, with flanking paths shown

The arrangement of acoustically lined duct and reverberant enclosure is shown in Figure 6. The breakout/breakin and direct structural flanking paths are shown. This situation is about the most basic that can be considered, whilst still retaining the essential features of the flanking processes. Coupled structural/acoustic waves in the lined duct are modelled by the use of a Rayleigh-Ritz variational formulation involving three structural degrees of freedom and three acoustic degrees of freedom. This model can accommodate both "predominantly acoustic" coupled modes, where most of the power flow is in the fluid contained in the duct, and "predominantly structural" coupled modes, in which most of the power flow is in the duct walls. The latter type of mode is responsible for direct structural flanking, while the former mode type can play its part in the breakout/breakin or radiation bypass flanking mechanism. (Astley is responsible for the main part of the theoretical formulation.)

Acoustic breakout is modelled in much the same way as was outlined in Section 2.2. Modelling breakin directly is less straightforward, so instead the acoustic Principle of Reciprocity is employed, with a point monopole within the duct as shown in Figure 6 and an observer in the reverberant sound field within the enclosure. A series of coupled modes (of both the predominantly acoustic and predominantly structural types) is matched to this point source by using appropriate matching conditions and a weighted residual procedure. This ensures that both flanking mechanisms are included in the formulation. It is straightforward to compute the mean squared sound pressure in the reverberant sound field surrounding the duct if the direct sound field contribution from the duct radiation is neglected. (Otherwise the direct field could be included, but at the expense of a considerably more involved analysis.) When the source and observer points are interchanged, the acoustic breakin sound pressure level from the reverberant sound field is readily calculated.

2.3.2 Some typical results for flanking transmission in a square section duct

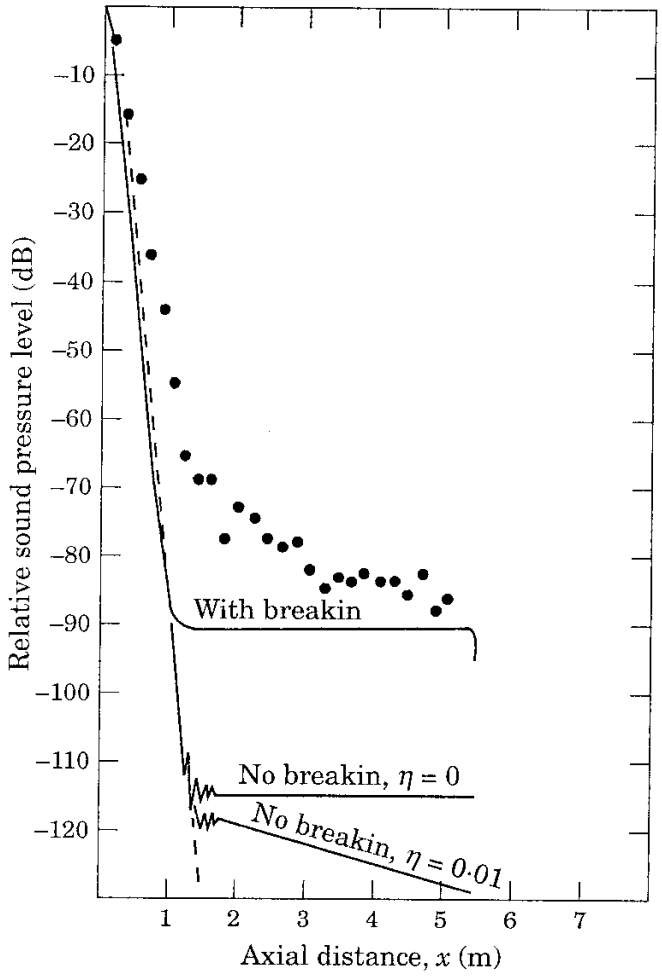

Figure 7. Axial sound pressure level distribution at 1.6kHz in a 300mm square section duct with 0.58mm galvanized steel walls, having a 53mm glass fibre lining on all four walls; ——, predicted sound level in flexible walled duct with all mode types; — —, predicted from least attenuated mode only; ●, measured data.

Some representative predicted and measured results are shown in Figure 7, for a frequency of 1.6 kHz. This frequency was chosen because it is close to the peak in both the measured and predicted attenuation rate along the duct, and would therefore be likely to demonstrate flanking effects most effectively. The predicted attenuation rate is rather higher than that evident in the measured data mainly because, at this frequency, the number of degrees of freedom in the trial function used in the Rayleigh-Ritz formulation gives rather limited resolution of the structural/acoustic mode shapes, and correspondingly of the axial wavenumber. Even so, the agreement is reasonable. However, the main points to be noted are:

(i) the sound pressure level falls off linearly with distance up to about x = 1m, after which it starts to level off and reaches an almost constant value at $x \approx 3.5$m
(ii) for distances greater than about 1m from the source, the least attenuated mode assumption is profoundly unsatisfactory in predicting the axial sound pressure pattern
(iii) where breakin is neglected, the predominantly structural mode does create a plateau caused by direct structural flanking only, but at far too low a level; and the value of the structural loss factor η determines the axial decay rate of this "structural" type mode (the undulations at the beginning of the plateau region are interference patterns between the "acoustic" and "structural" mode types, since they have similar magnitudes at this point)
(iv) the prediction including breakin, taking into account all mode types, agrees best with the measured data and offers convincing evidence supporting the assumptions on which the model is based.

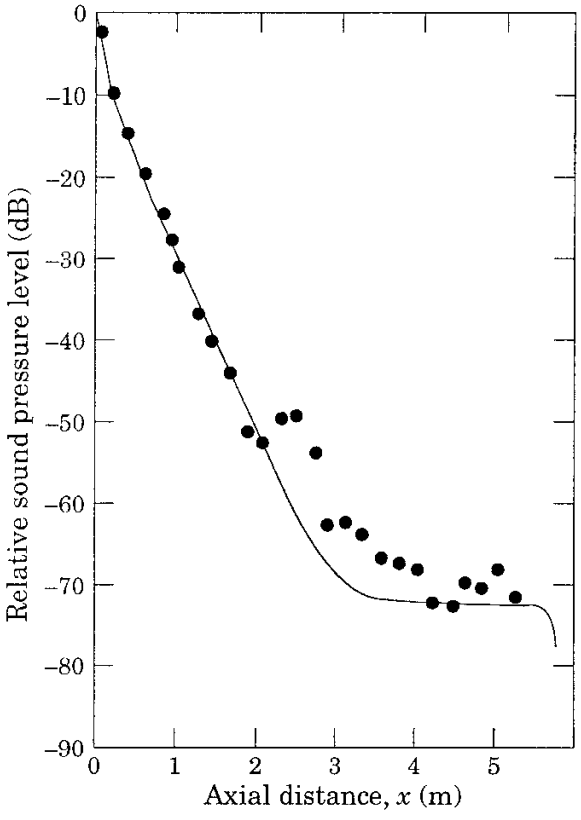

Figure 8. Axial sound pressure level distribution at 500 Hz in the experimental duct of Figure 7; ——, predicted sound level in flexible walled duct with all mode types, including breakin; ●, measured data.

Predicted and measured data for the above duct at a frequency of 500 Hz are plotted in Figure 8. At this lower frequency, the trial function is much better able to cope with the mode shapes etc., and agreement between prediction and measurement is quite acceptable.

3 BENIGN ASPECTS OF DUCT WALL BREAKOUT

In this section the two useful manifestations of duct wall breakout, previously mentioned, are discussed.

3.1 "Natural" attenuation in unlined ducts

3.1.1 A predictive model

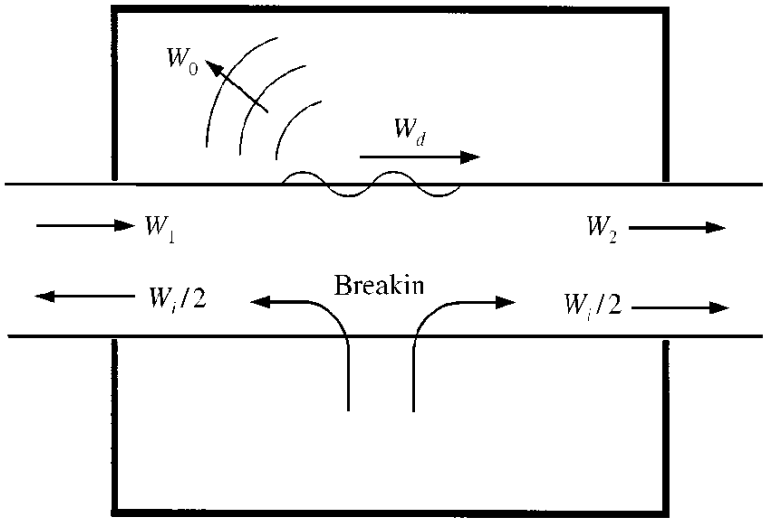

Figure 9. Power flow in an unlined duct passing through a reverberant enclosure.

This problem was suggested to the author by Ballagh[24] and the results of an investigation were reported by Cummings[7]. The duct arrangement is shown in Figure 9. An unlined duct passes through a reverberant enclosure, and sound power W_1 enters the duct from the left. Sound power W_d is lost by dissipation caused by structural damping in the duct walls, and breakout sound power W_0 is transmitted into the reverberant enclosure. Breakin sound power W_i enters the duct, splitting equally between inlet and outlet, and the remainder of W_1 ($W_2 = W_1 - W_0 - W_d$), together with $W_i/2$, leaves the duct to the right. The treatment of this problem is somewhat akin to the flanking problem in Section 2.3, though it is considerably less complicated because (i) there is no internal acoustic lining in the duct, and (ii) there is no need to account for "structural" type modes in the duct (even though they would exist), since they would play only a small part in the breakout process.

Sound power balance equations are established, and solved by means of a somewhat involved iterative process. The Principle of Reciprocity is (as in the flanking problem) again employed to find the breakin sound power straightforwardly. There is a net attenuation of sound within the duct from inlet to outlet, since a part (W_d) of W_1 is lost to structural damping in the duct walls and a further loss (W_0) occurs by breakout. Only a part (W_i) of this returns to the duct interior, and of this only half leaves via the duct outlet. It is assumed in the formulation[7] that the axial decay rate of sound power within the duct is constant along the length, though in reality this would be unlikely to be the case. Not only the structural loss factor of the duct wall, but also the absorption characteristics of the surrounding reverberant space, are taken into account in the predictive method, which enables the average axial loss in sound power in dB/unit distance to be found.

3.1.2 Representative results

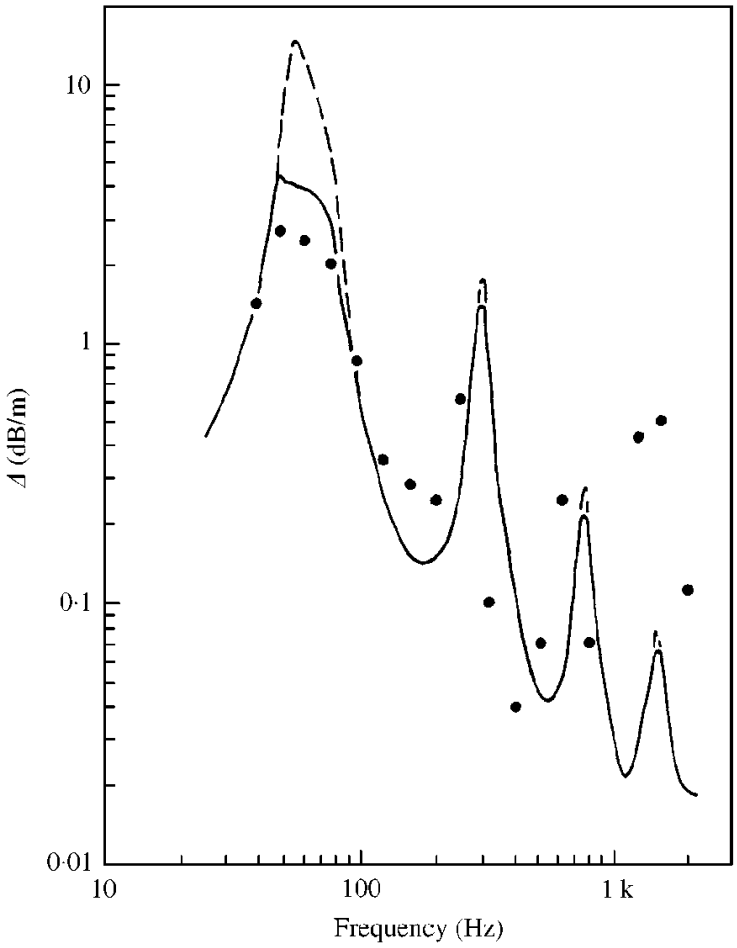

Figure 10. Natural attenuation rate in a 300mm square duct with 0.91mm galvanized walls; ——, predicted attenuation rate with breakin, η = 0.15; — —, predicted attenuation rate without breakin, η = 0.15; ●, measured data (Nelson and Burnett[25]).

Some illustrative results, plotted as attenuation rate Δ (in dB/m) *versus* frequency, are shown in Figure 10. The experimental data were taken by Nelson and Burnett[25], and appear to be unique among unlined duct attenuation measurements in that the reverberation times of the test chamber were recorded. Consequently, these data were suitable for comparison to results from the predictive method employed, since this required knowledge of the "room constant". It should be noted that natural duct attenuation was not the phenomenon primarily studied by Nelson and Burnett, and that it is, to some extent, fortuitous that their data can be used to infer values of natural duct attenuation. (It is also, no doubt, a result of meticulousness in their recording of relevant data.)

The most obvious feature of the results in Figure 10 is the series of very prominent peaks in Δ, at frequencies which – not surprisingly – turn out to correspond to transverse resonance frequencies of the duct walls. The highest peak is around 50 Hz, and the measured peak attenuation rate is about 2.8 dB/m, with the predicted figure (with breakin) being about 4.3 dB/m. The agreement between these values is good, considering that the measured data were not specifically intended to be used for this purpose. Without breakin, the predicted peak attenuation is about 15 dB/m,

illustrating the very significant effect of breakin – together with the absorption characteristics of the enclosure – at this particular frequency.

A salient point here is that dissipative silencers of the type commonly used in HVAC duct systems would only have an insertion loss of about the same magnitude – at this frequency – as that afforded by the unlined duct in this situation! At the lowest duct wall resonance frequency, there is a quite respectable natural attenuation rate over a frequency range of about one octave. And this is at no extra cost. Admittedly, the natural attenuation rate tends to fall off as the frequency rises, though the peak values are still significant. However, the acoustical engineer involved in the design of HVAC systems can, in principle, select duct configurations (the two transverse dimensions and wall thickness, for a given duct material, being design parameters) to give low frequency peaks in duct attenuation where they are needed. Clearly, this should not be done at the expense of (say) office personnel who happen to work in a building space selected for a high degree of breakout absorption – plant rooms would be much more appropriate.

3.2 Breakout and attenuation effects in permeable-walled hoses

Woven fabric hoses with porous walls are manufactured by various companies such as Westaflex in France and Nihon Sekiso in Japan. They are widely used – as mentioned in the Introduction – in the air intake systems of automobile engines. Significant sound power is actually dissipated in the walls of these hoses, as was shown by Cummings and Kirby[26]. And some of the sound power incident from the engine is radiated to the exterior. The author has heard a rather cynical suggestion that this feature might be advantageous in intake noise test methods where the intake noise is measured at a given distance from the air inlet, since a part of the intake sound power emanating from the engine could then be radiated, through the tube wall, farther from the measuring microphone than the air inlet! It is, perhaps, unlikely that this is the main reason for the popularity of porous hoses, since radiation from the duct wall is likely to be somewhat directional, toward the air inlet (see that results of Cummings[18]), and this effect could cancel that of distance. In any case, the radiated sound power levels appear to be significantly smaller than the incident levels.

The prediction of the acoustic performance of porous hoses is dependent on knowledge of the wall impedance as a function of frequency. This is difficult to measure directly, as concluded by Park, Ih, Nakayama and Kitahara[27], who investigated measurement techniques in detail and presented their own model for prediction of the *TL* of these tubes. Park, Ih, Nakayama and Takao[28] also reported an "inverse estimation procedure" for the wall impedance of porous hoses. By contrast, the wall impedance in the work of Cummings and Kirby[26] was derived by a rather crude procedure whereby the wall impedance used to predict the axial sound pressure distribution measured in a porous tube was adjusted to yield a "best fit" to measured data.

3.2.1 A predictive model

The predictive model of Cummings and Kirby[26] will be briefly described here, since it is more comprehensive that that of Park, Ih, Nakayama and Kitahara[27]. In the former model the external sound field is coupled to the sound field inside the porous tube, whereas in the latter formulation, the external radiation impedance is ignored. In the model of Cummings and Kirby, the sound field within the tube is divided axially into "cells", and conditions of continuity of acoustic force and volume velocity between cells are imposed. The sound pressure in each cell is assumed axisymmetric and is represented, in the usual way, by a zero order Bessel function. The exterior radiation impedance surrounding the cells is, however, permitted to differ between cells to allow for the radiation interaction between cells (modelled by a mutual radiation impedance formulation). Consequently, the interior wall impedance on the cell surfaces varies along the tube even though the impedance of the tube wall (defined as the quotient of sound pressure differential and the inner/outer average radial particle velocity, divided by the characteristic impedance of air) is constant along the tube. (It is assumed here that the tube wall can be assumed to have an impedance that is independent of its extent and mounting conditions, i.e., it behaves as though it is permeable but structurally rigid.) An iterative scheme is employed to find the internal sound pressure distribution inside the tube. At the first step, the exterior sound pressure is assumed zero,

and the interior sound field is found. An approximate distribution of the exterior sound pressure is then found, and this is used in the next step to refine the interior sound field. This process is continued until the solution converges. It is possible to neglect coupling effects between the interior of the tube and the exterior region by simply putting the external sound pressure equal to zero, i.e., truncating the iteration process after the first step.

Sound power flows and a control volume (delineated by the dashed line) are indicated in Figure 11, in a system where sound is incident from a source at the right-hand end of a porous tube, which is terminated by a ρc impedance (in the form of a semi-infinite rigid tube) at its left-hand end. One may write sound power balance equations:

$$W_{inc} = W_i - W_r - W_t \; ; \quad W_{diss} = W_{inc} - W_{rad} \; . \qquad (4a,b)$$

Here, W_i is the incident sound power, W_r the reflected power, W_{inc} the power incident on the tube walls from the inside, W_{rad} the externally radiated power, W_t the power transmitted toward the termination and W_{diss} the sound power dissipated in the walls of the porous tube.

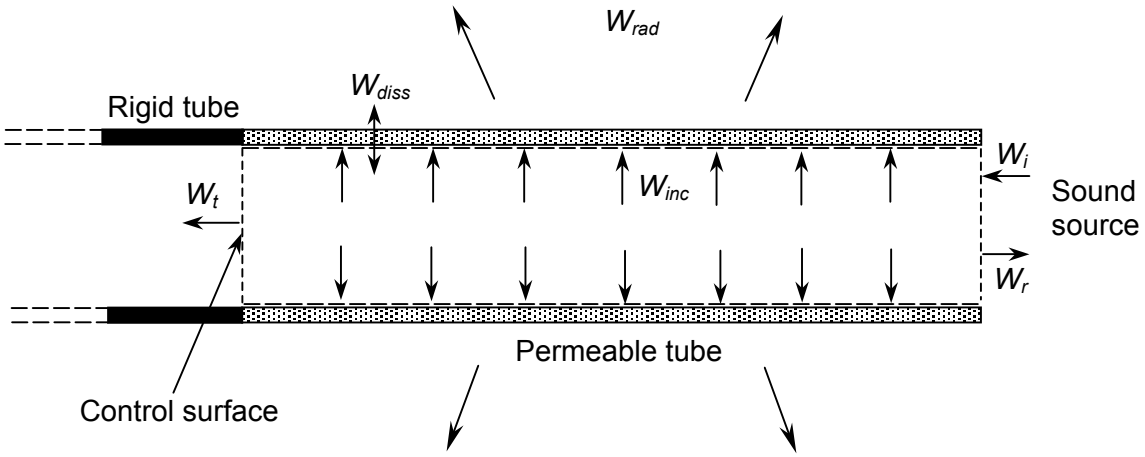

Figure 11. Power flow components in a section of permeable-walled tube.

Two *TL* definitions would seem to be appropriate here:

$$TL = 10 \log(W_i / W_t) \quad \text{and} \quad TL = 10 \log[W_i / (W_{rad} + W_t)] \; . \qquad (5a,b)$$

Definition (5a) relates the transmitted sound power, in the tube, to the incident sound power and is a measure of the effectiveness of the porous tube as a silencer, without reference to the radiated sound power. Definition (5b) takes account of both internally transmitted and radiated sound power. The usual breakout *TL* definition appears to be of lesser interest in this context.

In the work of Cummings and Kirby[26], a perforated aluminium tube was studied in order to verify the predictive model, prior to investigations of representative porous fabric tubes. The wall impedance of the aluminium tube, as a function of frequency, could be calculated to good accuracy, thereby removing one possible source of uncertainty in comparisons between theory and measurement. Predicted and measured data of the internal sound pressure distribution were in excellent agreement for the aluminium tube.

3.2.2 Some results

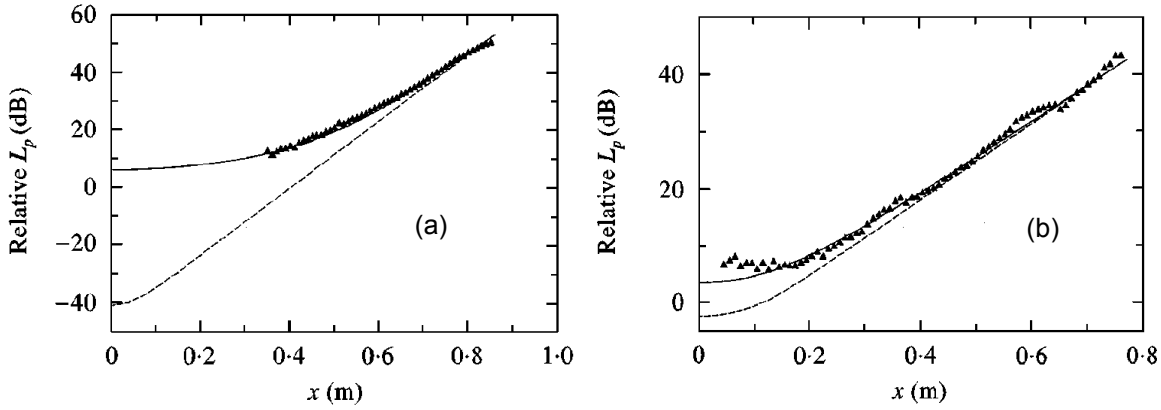

Figure 12. Predicted, —— (with coupling to the external sound field), - - - - - (without coupling to the external sound field), and measured, ▲ , axial sound pressure distributions in (a) the aluminium tube at 200 Hz, (b) the porous fabric tube at 250 Hz.

In Figure 12 are shown predicted and measured data of the sound pressure inside the aluminium tube and a typical porous fabric tube. The sound was injected at one end of the tube, and the other end was terminated by a rigid plate. The coordinate x in both plots is the distance from the rigid plate to the measurement point in the tube. The predicted curve in the case of the fabric tube is based on the "best fit" wall impedance, whereas the appropriate theoretical value of the (space-averaged) wall impedance of the aluminium tube was used. Predicted curves both with and without coupling to the external sound field are plotted. It can be seen that internal/external coupling is very important in the case of the aluminium tube, and that taking this into account yields excellent agreement between prediction and measurement. Internal/external coupling is much less important in the case of the fabric tube, though it is not completely insignificant. In fairly short tubes, it is probably justifiable to neglect it for typical materials, as was done by Park, Ih, Nakayama and Kitahara[27]. Agreement between the predicted and measured sound pressure pattern in the fabric tube is good, given that considerable inhomogeneity in the wall impedance would be expected in this type of material[27].

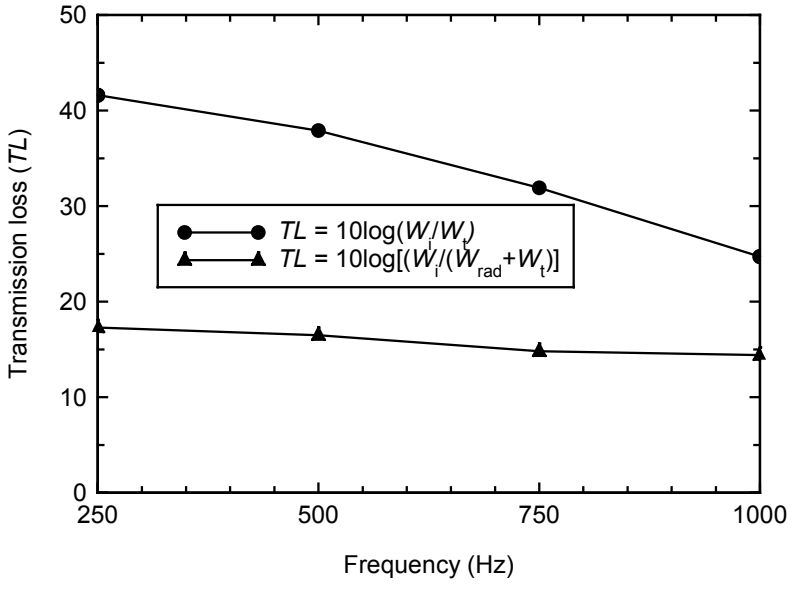

Figure 13. Predicted transmission loss, according to two definitions, for a porous hose.

Calculated *TL* plots – from equations 5(a,b) – are shown, for the porous hose (of length 776mm), in Figure 13. It can be seen that the hose is very effective as a duct silencer, particularly at the lower frequencies, where the *TL* from equation (5a) exceeds 40 dB. The *TL* values from equation (5b) are lower, but are actually an indication of the extent of power *dissipation* in the tube walls, since W_{rad} + W_t is a measure of the difference between the *net* incident power, $W_i - W_r$, and W_{diss}. If $W_{diss} \rightarrow W_i - W_r$, then $TL \rightarrow \infty$. One can see, from equations (4a,b) and the lower plot in Figure 13, that by far the greater part of W_i is dissipated in the duct walls. This is an indication of the effectiveness of porous tubes as duct silencers.

4 CONCLUSIONS

In the various – rather specialized – types of duct and applications described in this paper (all of which involve acoustic breakout effects), there are many very interesting physical phenomena evident: for example, the vibration of (in some cases) rather complicated structures such as flat-oval ducts and distorted circular ducts, structural/acoustic interaction, coupled structural/acoustic modes, sound radiation from structures with (in some cases) complex vibration patterns or acoustic source distributions and breakin transmission from reverberant spaces to ducts. There is also a varied range of mathematical techniques appropriate to the prediction of the various effects of interest (breakout *TL*, radiation efficiency, duct attenuation, etc.): approximate analytical solutions for idealized systems, variational techniques, numerical methods for field problems such as finite element methods and finite difference approximations, Gaussian quadrature in both finite element methods and the integrations required in radiation problems.

Fairly basic predictive methods can, in many cases, give surprisingly accurate results which are sufficient for most engineering design purposes. These are, however, at their best when based on more complete models which can be systematically simplified.

On the basis of the evidence presented here, there is little doubt that duct wall breakout is more often a problem than a benefit. However, a quantitative understanding of the various phenomena involved can enable the nuisance aspects of breakout to be minimised or even completely eliminated. And there are certain situations or applications in which breakout – and/or its associated effects – can be exploited, by careful design in an economical way, to bring about very worthwhile degrees of noise reduction.

ACKNOWLEDGMENTS

The author has been very fortunate, in his career, to work in collaboration with some very talented individuals, notably Prof. Jeremy Astley, who has made major contributions to a variety of joint research projects and from whom a great deal has been learned. Also several young researchers, particularly Dr. Ing-Juin Chang and Dr. Ray Kirby, have made extensive and very valuable contributions to much of the research cited in this paper.

5 REFERENCES

1. C.H. Allen. Noise Reduction (Editor L. L. Beranek), McGraw-Hill, 550-553. (1960).
2. I. Sharland. Woods Practical Guide to Noise Control, Woods Acoustics, 107-108. (1972).
3. J.D. Webb. Noise Control in Mechanical Services, Sound Attenuators Ltd., Sound Research Laboratories Ltd., chapter 9. (1972).
4. D.A. Wilbur and R.F. Simmons, 'Determining sound attenuation in air conditioning systems', Heating, Piping and Air-Cond. 14 317-321. (1942).
5. C.F. Piestrup and J.E. Wesler, 'Noise of ventilating fans', J. Acoust. Soc. Am. 25 322-326. (1953).

6. W.F. Kerka, 'Attenuation and generation of sound in elbows with turning vanes', Trans. A.S.H.R.A.E. 66 129-153. (1960).
7. A. Cummings, 'The attenuation of sound in unlined ducts with flexible walls', J. Sound Vib. 174 433-450. (1994).
8. R. Kirby and A. Cummings, 'Structural/acoustic interaction in air-conditioning ducts in the presence of mean flow', Proc. ISMA23, Leuven. (September 1998).
9. A. Cabelli, 'Application of the time dependent finite difference theory to the study of sound and vibration interactions in ducts', J. Sound Vib. 103 13-23. (1985).
10. R. J. Astley and A. Cummings, 'A finite element scheme for acoustic transmission through the walls of rectangular ducts: comparison with experiment', J. Sound Vib. 92 387-409. (1984).
11. A. Cummings, I.-J. Chang and R. J. Astley, 'Sound transmission at low frequencies through the walls of distorted circular ducts', J. Sound Vib. 97 261-286. (1984).
12. P.G. Bentley and D. Firth, 'Acoustically excited vibrations in a liquid-filled tank', J. Sound Vib. 19 179-191. (1971).
13. S.N. Yousri and F.J. Fahy, 'Distorted cylindrical shell response to internal acoustic excitation below the cut-off frequency', J. Sound Vib. 52 441-452. (1977).
14. A. Cummings and I.-J. Chang, 'A finite difference scheme for acoustic transmission through the walls of distorted circular ducts and comparison with experiment', J. Sound Vib. 104 377-393. (1986).
15. A. Cummings and I.-J. Chang, 'Noise breakout from flat-oval ducts', J. Sound Vib. 106 17-33. (1986).
16. A. Cummings and R. Kirby, 'Low frequency sound transmission in ducts with permeable walls', J. Sound Vib. 226 237-251. (1999).
17. G.L. Brown and D.C. Rennison, 'Sound radiation from pipes excited by plane acoustics waves', Proc. Noise, Shock and Vib. Conference, Melbourne, 416-425. (1974).
18. A. Cummings, 'Low frequency acoustic radiation from duct walls', J. Sound Vib. 71 201-226. (1980).
19. A. Cummings, 'Higher order mode acoustic transmission through the walls of rectangular ducts', J. Sound Vib. 90 193- 209. (1983).
20. A. Cummings, 'Approximate asymptotic solutions for acoustic transmission through the walls of rectangular ducts', J. Sound Vib. 90 211-227. (1983).
21. I.L. Vér, 'A review of the attenuation of sound in straight lined and unlined ductwork of rectangular cross-section', Trans. A.S.H.R.A.E. 84 122-149. (1978).
22. F.P. Mechel, 'Design criteria for industrial mufflers', Trans. Inter-Noise 75, 751-760. (1975).
23. A. Cummings and R. J. Astley, 'The effects of flanking transmission on sound attenuation in lined ducts', J. Sound Vib. 179 617-646. (1995).
24. K.O. Ballagh, personal communication. (1992).
25. P.A. Nelson and R. Burnett, 'Laboratory measurements of breakout and break-in of sound through walls of rectangular ducts', Sound Attenuators Ltd. Tech. Rept. No. TRC 107. (1981).
26. A. Cummings and R. Kirby, 'Low frequency sound transmission in ducts with permeable walls', J. Sound Vib. 226 237-251. (1999).
27. C.-M. Park, J.-G. Ih, Y. Nakayama and S. Kitahara, 'Measurement of acoustic impedance and prediction of transmission loss of the porous woven hose in engine intake systems', Appl. Acoust. 63, 775-794. (2002).
28. C.-M. Park, J.-G. Ih, Y. Nakayama and H. Takao, 'Inverse estimation of the acoustic impedance of a porous woven hose from measured transmission coefficients', J. Acoust. Soc. Am. 113, 128-138. (2003).